Finite Element Analysis of Steel Tube Bundle Composite Shear Wall with Different Constructions

Shengwu Wan and Xueyuan Cheng

Abstract In order to study the seismic performance of the steel tube bundle composite shear wall with different constructions. Based on the failure tests of three composite shear wall specimens without steel tube bundle end, with studs and stiffener, a feasible numerical model is established by ABAQUS. The hysteresis curve and energy dissipation coefficient, skeleton curve and ductility of the shear wall were further analyses by varying the axial compression ratio and the spacing of the internal diaphragm. The results show that the stud group and the stiffener group can effectively improve the horizontal bearing capacity, energy dissipation capacity, bearing capacity and ductility of the shear wall. Under the condition of low axial compression ratio, the horizontal bearing capacity of the member with stud is increased by 6.3%; Under the condition of high axial compression ratio, the horizontal bearing capacity of members with stiffeners is increased by 4.5%; The change of axial compression ratio and the spacing between inner diaphragms of shear walls with stiffeners has little effect on their energy dissipation capacity and ductility.

Keywords Steel tube bundle composite shear wall · Seismic performance · Finite element simulation · Inner spacer spacing · Axial compression ratio

1 Instruction

Compared with ordinary reinforced concrete members, steel tube bundle composite shear wall, as a new type of shear wall member, has higher bearing capacity and energy consumption capacity, and is suitable for standardized design, factory production and assembly construction.

Wu et al. [1], Huang et al. [2] studied the double steel plate shear wall with structural measures through axial compression test and quasi-static test, and concluded that the ductility of the shear wall with structural measures under periodic load is

S. Wan · X. Cheng (✉)
School of Urban Construction, Wuhan University of Science and Technology, Wuhan, Hubei, China
e-mail: 599282382@qq.com

S. Wang et al. (eds.), *Proceedings of the 2nd International Conference on Innovative Solutions in Hydropower Engineering and Civil Engineering*, Lecture Notes in Civil Engineering 235, https://doi.org/10.1007/978-981-99-1748-8_25

higher than that of the general shear wall structure. Takeuchi et al. [3], Yan [4, 5], Ozaki [6], etc. have studied the influence of steel plate spacing, thickness, etc. On the shear wall components of steel plate shear wall components with structural measures through experiments. The latest research status in China mainly focuses on the seismic performance [7, 8], shear performance [9] and compression bending performance [10] of steel tube bundle composite shear wall, and the research on structural measures [11, 12] is less.

In this paper, based on ABAQUS, the steel tube bundle composite shear wall with stud and stiffener at the end is simulate the low-reversed loading tests., and the feasibility of the model is verified by comparing the hysteresis curves of simulation and test. Further changing the axial compression ratio and the spacing between inner diaphragms of steel tube bundle composite shear walls, the influence of various parameters on the seismic performance of steel tube bundle composite shear walls with different structures is analyzed.

2 Overview of Model Design

Three groups of 9 test pieces are designed, Control group (steel tube bundle composite shear wall), shear bolts group (set the specification of two rows to A8* 40 mm@120 mm shear bolts) and stiffeners group (set two groups of 30 * 3 mm stiffeners and arrange them in full length). Among them, each group is also provided with a reference specimen with different axial compression ratio and spacing between inner diaphragms. See Table 1 for dimensions of each test piece. In the finite element simulation, the material properties, specimen size and loading method in the test in literature [12] are adopted.

3 Establishment and Verification of Finite Element Model

3.1 Material Constitutive Relation

The ideal elastic–plastic constitutive relation double line model is adopted for steel. The model assumes that the steel is isotropic and satisfies Mises yield. The elastic modulus of steel is E_s = 2.03e5 MPa, Poisson's ratio is 0.3. Considering that the outer steel plate of this model has a restraining effect on the internal concrete and the outer steel plate is rectangular, the constitutive relation of confined concrete is used. The stress–strain relationship of concrete under compression is taken as per [13].

The concrete damage model established in this damage model of concrete by Lubliner [14] and Lee [15], the elastic stiffness degradation caused by concrete damage is described by damage factors (dc, dt).

Table 1 Design parameters of each component

Group	Model no	Axial compression ratio	Wall section size
Blank	CSW1	0.3	103 * (100 + 180 * 3 + 100)
	CSW1-1	0.1	103 * (100 + 180 * 3 + 100)
	CSW1-2	0.3	103 * (100 + 90 * 6 + 100)
Stud	CSW2	0.3	103 * (100 + 180 * 3 + 100)
	CSW2-1	0.1	103 * (100 + 180 * 3 + 100)
	CSW2-2	0.3	103 * (100 + 90 * 6 + 100)
Stiffener	CSW3	0.3	103 * (100 + 180 * 3 + 100)
	CSW3-1	0.1	103 * (100 + 180 * 3 + 100)
	CSW3-2	0.3	103 * (100 + 90 * 6 + 100)

3.2 Unit Selection and Meshing

All grids in the model are structured, C3D8R concrete and C3D81 steel pipe bundle, it can effectively avoid shear self-locking and excessive deformation. The global size of the mesh is 120 mm. The stud is shear bolts as a non independent entity to grid it, meshing is C3D8R and the approximate global size is 1 mm.

3.3 Contact Treatment and Boundary Conditions

In the model, the steel tube bundle, loading beam and foundation slab are considered as a whole, so there is no contact between them. The normal behavior of the contact property between the steel tube bundle and the filled concrete is defined as hard contact, the tangential behavior is defined as penalty contact, and the friction coefficient is taken as the reference value of 0.6. The stiffener is set to be embedded in the concrete in a built-in coupling mode. The stud is embedded into the filled concrete of the steel tube bundle in a built-in coupling mode.

According to the test method, the boundary condition of the model is that the foundation plate is set as fully consolidated, the reference point is set at the centroid position on the right side of the loading beam, the reference point is coupled with the entire end face on the left side of the loading beam, and the low circumferential

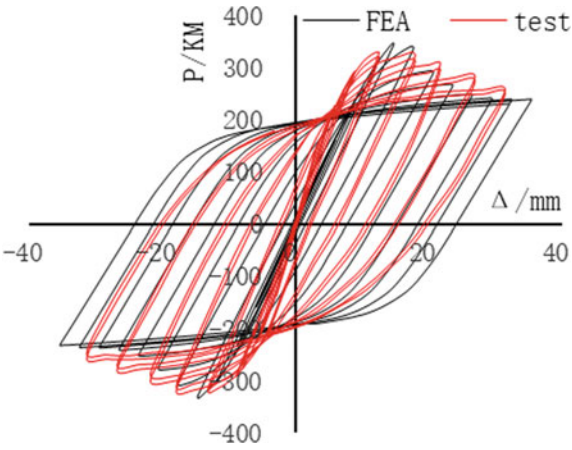

Fig. 1 CSW1 hysteretic curve comparison between test and finite element simulation

displacement load acts on this reference coupling point. A reference point is set above the loading beam and coupled with the upper end face of the loading beam. The axial pressure acts on this reference coupling point.

3.4 Finite Element Model Verification

Use the above modeling methods to model and analyze CSW1, CSW2, and CSW3, and compare the finite element simulation results of the hysteresis curve with the experimental results. The results are shown in Fig. 1. It can be seen from Fig. 1 that the shape of the hysteresis curve obtained by numerical simulation and test is similar, and the change rule of the curve is also the same, except that the curve values are different. The error of the ultimate load is within 5% and the simulation result is higher than the test result, because the finite element model is the ideal model of the test, and the bond slip between the steel tube bundle and the core concrete is not considered.

4 Finite Element Simulation Results and Analysis

4.1 Hysteresis Curve and Energy Dissipation Capacity

In order to further accurately analyze the influence of axial compression ratio and spacing of inner diaphragms on the energy dissipation capacity of steel tube bundle

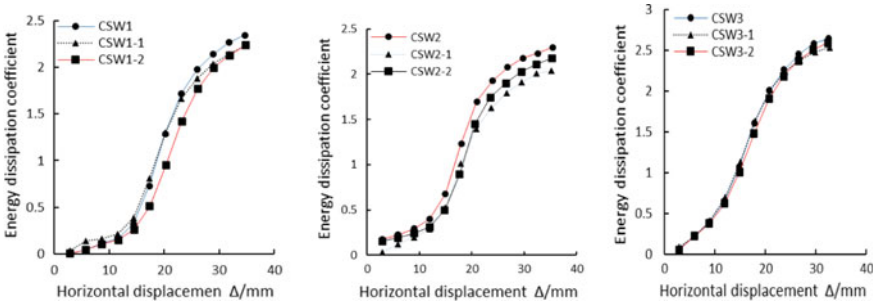

(a) blank (b) stud (c) stiffener

Fig. 2 Energy dissipation coefficient—displacement diagram

composite shear wall with different structural measures, energy dissipation coefficient is used to measure. See Fig. 2 for the energy dissipation coefficient displacement diagram of 9 test pieces.

It can be seen from Fig. 2 that by comparing the blank group, shear bolts and stiffeners with changed axial compression ratio, it can be seen that when the axial compression ratio decreases, the energy dissipation coefficient decreases, indicating that the energy dissipation capacity decreases. By comparing the shear wall groups with different structures in each group, it can be found that the energy change curves of the blank group and shear bolts are quite different, which indicates that changing the axial compression ratio and the spacing of inner diaphragms has a greater impact on the energy dissipation coefficients of the blank group and the stud group. The energy dissipation coefficients of the three specimens of the stiffening group are greater than 2.5. The energy dissipation capacity of the stiffening group is stronger than that of the other groups, and the axial compression ratio and the spacing of inner diaphragms have little influence on it.

4.2 Skeleton Curve and Bearing Capacity

It can be seen from Fig. 3 that when the axial compression ratio decreases and the spacing between inner diaphragms remains unchanged, the slope of the curve descent section of the blank group and shear bolts group becomes smaller, and the trend tends to be flat. The ductility of the specimen increases. However, the curve of stiffening rib group did not change significantly, and the ductility did not improve significantly. When the spacing between inner diaphragms decreases and the axial compression ratio remains unchanged, the ductility of blank group and shear bolts group increases, while that of stiffener group does not change significantly.

It can be seen from Table 2 that when the axial compression ratio decreases and the spacing between inner diaphragms remains unchanged, the ultimate load of the blank group decreases by 3.66%, the ultimate load of the shear bolts group decreases

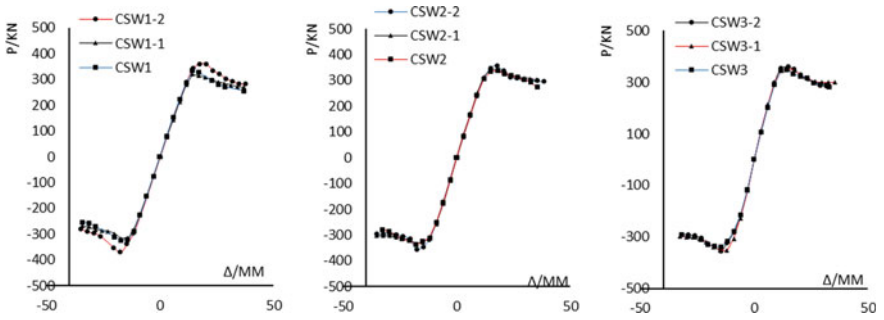

(a) blank (b) stud (c) stiffener

Fig. 3 Skeleton curves of each group

by 2.37%, and the ultimate load of the stiffener group decreases by 0.70%; It shows that the change of axial compression ratio has influence on the ultimate bearing capacity of blank group and stud group, and the influence on the ultimate bearing capacity of shear wall with stiffening at the edge can be ignored. When the spacing between the inner diaphragms decreases and the axial compression ratio remains unchanged, the ultimate bearing capacity of the blank group increases by 12.06%, the ultimate bearing capacity of the shear bolts group increases by 6.39%, and the ultimate bearing capacity of the stiffener group increases by 4.50%; It shows that the increase of embedded steel plates will improve the ultimate bearing capacity of shear walls in varying degrees, and the blank group has the greatest impact.

Table 2 Mechanical properties parameters

Model No	P_y/kN	Δ_y/mm	P_u/kN	Δ_u/mm	μ
CSW1	283.53	10.31	315.07	27.02	2.62
CSW1-1	272.49	10.24	303.96	31.45	3.07
CSW1-2	306.20	10.43	340.62	33.49	3.21
CSW2	293.25	9.28	320.29	33.76	3.15
CSW2-1	286.42	9.15	312.59	34.29	3.70
CSW2-2	304.32	9.96	332.57	37.94	3.80
CSW3	299.26	8.65	323.42	29.66	3.40
CSW3-1	296.53	8.37	321.16	29.80	3.56
CSW3-2	305.58	9.74	335.91	29.86	3.46

4.3 Ductility

In this paper, displacement ductility coefficient is used μ to represent the ductility of shear walls with different structures at the edges, which is expressed as $\mu = \Delta_u/\Delta_y$. See Table 2 for displacement ductility coefficient of each specimen.

It can be seen from the displacement ductility coefficient in Table 2 that when the axial compression ratio decreases and the spacing between inner diaphragms remains unchanged, The ultimate bearing capacity of CSW1-1 is less than that of CSW1, but its displacement ductility coefficient is 17.18% higher than that of CSW1; At the same time, the ultimate bearing capacity of CSW2-1 is lower than that of CSW2, but its ductility coefficient is 18.97% higher than that of CSW2; The ductility coefficient in the stiffening rib group is increased by 4.70%. Blank group and stiffening group can improve the ductility of steel tube bundle composite shear wall by reducing the axial compression ratio. When the distance between inner diaphragms decreases and the axial compression ratio remains unchanged, the displacement ductility coefficient increases. The displacement ductility coefficient of CSW1-3 is 22.52% higher than that of CSW1, and that of CSW3-2 is 1.7% higher than that of CSW3. It shows that increasing the number of internal diaphragms can significantly improve the ductility of blank group and shear bolts group.

5 Conclusion

(a) The ductility of the three groups of steel tube bundle composite shear walls in this paper can be improved to varying degrees by reducing the axial compression ratio. The ductility of the blank group and the stud group is significantly improved, and the energy dissipation coefficient is reduced, indicating that the energy dissipation capacity is reduced.

(b) The smaller the spacing between inner diaphragms, the more the ductility increases; The spacing of inner diaphragms has a great influence on the energy dissipation coefficient of blank group and stud group, and the ultimate bearing capacity has been improved to varying degrees, among which the blank group has the largest influence.

(c) The energy dissipation capacity of steel tube bundle composite shear wall structure with stiffening rib structure mechanism is better than blank group and stud group, and the change of axial compression ratio and inner diaphragm spacing has little effect on its energy dissipation capacity.

References

1. Wu XD, Tong LW, Xue WC (2016) Experimental investigation on seismic behavior of short-leg steel-concrete-steel composite shear walls. J Tongji Univ (Nat Sci Ed) 44(09):1316–1323
2. Huang ST, Huang YS, He A (2018) Experimental study on seismic behaviors of an innovative composite shear walls. J Constr Steel Res 148:165–179
3. Takeuchi M, Narikawa M, Matsuo I (1998) Study on a concrete filled structure for nuclear power plants. Nucl Eng Des 179(2):209–223
4. Yan JB, Wang XT, Wang T (2018) Compressive behaviors of normal weight concrete confined by the steel face plates in SCS sandwich walls. Constr Build Mater 171:437–454
5. Yan JB, Wang XT, Wang T (2018) Seismic behaviors of double skin composite shear walls with overlapped headed studs. Constr Build Mater 191:590–607
6. Ozaki M, Akita SO, Suga H (2004) Study on steel plate reinforced concrete panels subjected to cyclic in-plane shear. Nucl Eng Des 228(1):225–244
7. Yu HR, Wang Y, An Q (2021) Seismic performance analysis of anchored prefabricated wall beam connection of steel tube bundle composite shear wall structure. Ind Build 51(06):84–94
8. Zhang P, Zhou XG, Miao ZH (2020) Experimental study on seismic behavior of composite shear wall with bundled steel tube and infill concrete when shear span ratio is 1.5. Build Struct 50(5):109–115
9. Miao ZH, Zhou XG, Zhang P (2018) Simulation analysis on shear resistance of steel tube-concrete composite shear wall. J Yantai Univ (Nat Sci Eng Ed) 31(1):76–82
10. Zhao YF, Zhou XG (2022) Bending performance analysis of steel tube-concrete composite shear wall. J Yantai Univ (Nat Sci Eng Ed) 35(02):235–241
11. Song WG, Zhou XG, Zhao YF (2021) Compressive and bending performance of steel tube bundle-concrete composite shear wall and stiffeners on both sides of steel tube. J Yantai Univ (Nat Sci Eng Ed) 34(3):348–354
12. Wan SW, Xu P, Xu CX (2019) Experimental seismic behavior of steel tube bundle composite shear wall with different constructions. Sichuan Build Sci Res 45(4):18–23
13. Han LH (2016) Concrete filled steel tube structure. Science Press
14. Lubliner J, Oliver J, Oiler S, Onate E (1989) Plastic-damage model for concrete. Int J Solids Struct
15. Lee J, Fenves GL (1998) Plastic-damage model for cyclic loading of concrete structures. J Eng Mech Div ASCE 124(8):892–900